ISSN 0023-1584, Kinetics and Catalysis, 2009, Vol. 50, No. 6, pp. 892–898. © Pleiades Publishing, Ltd., 2009.
Original Russian Text © E.F. Sutormina, L.A. Isupova, A.N. Nadeev, V.A. Rogov, V.P. Ivanov, E.B. Burgina, A.A. Budneva, 2009, published in Kinetika i Kataliz, 2009, Vol. 50, No. 6, pp. 929–936.

Effect of the Reaction Medium on the Physicochemical Properties of the Oxide Monolith Catalyst IK-42-1 for Ammonia Oxidation

E. F. Sutormina, L. A. Isupova, A. N. Nadeev, V. A. Rogov, V. P. Ivanov, E. B. Burgina, and A. A. Budneva

Boreskov Institute of Catalysis, Siberian Branch, Russian Academy of Sciences, Novosibirsk, 630090 Russia

e-mail: selena@catalysis.ru

Received September 17, 2008

Abstract—The changes in the properties of the oxide monolith catalyst IK-42-1 for ammonia oxidation upon 3540-h-long operation as the second stage of a UKL-7 industrial reactor were studied by X-ray diffraction, chemical analysis, secondary ion mass spectrometry, temperature-programmed reduction, and IR spectroscopy. The spent catalyst shows a lower activity and a lower nitrogen oxide selectivity than the initial catalyst: the decrease in the NO yield is about 25%. As the catalyst operates, the state of its surface changes under the action of the reaction medium. The specific surface area of the catalyst decreases, and the total pore volume increases, which can cause a slight decrease in the ammonia conversion and diminish the mechanical strength of the monoliths. Under the ammonia oxidation conditions, there can be partial reduction of the catalyst surface and the local formation of a spinel structure (spinel-like defects). Oxygen adsorbed on these areas/defects is characterized by a high activation energy of desorption, which favors the reaction route yielding molecular nitrogen. According to IR spectroscopic data, the spent catalyst has a lower concentration of active, coordinatively unsaturated Fe^{2+} sites of adsorption, which are responsible for ammonia oxidation into NO. The decrease in the number of active sites can be due to both the breakdown of the solid solution of iron oxide in aluminum oxide during the reaction and the blocking of these sites by silicon, alkali and alkaline-earth metal, chromium, and rhodium atoms present on the surface of the spent catalyst.

DOI: 10.1134/S0023158409060160

The oxide monolith catalyst IK-42-1 for ammonia oxidation has been developed at the Boreskov Institute of Catalysis, Siberian Branch, Russian Academy of Sciences. The purpose of this catalyst is to replace part of the platinum group metal gauzes in the production of concentrated nitric acid and thus obtain a two-stage catalytic system in which this catalyst is used at the second stage [1]. The catalytic system consisting of nine gauzes and an oxide monolith bed instead of 12 gauzes is successfully employed in UKL-7 units operated at 0.716 MPa. The two-stage system for ammonia oxidation allows the initial weight of the platinum group metal catalyst to be reduced by 25–33% and the platinum metal losses be reduced by at least 15%. This system affords the same service life–average conversion of ammonia into nitrogen oxides as the pure platinum group metal catalyst [2]. Furthermore, the monolith catalyst makes the gas flow more uniform, thereby reducing the ammonia breakthrough, improving the explosion safety of the reactor, and extending the service life of the platinum group metal catalyst.

The monoliths generally do not undergo deformation or breaking under the action of the reaction medium during long-term operation of the oxide monolith catalyst. It was found by visual examination of spent monoliths that the catalyst surface has changed from brownish red to black. In addition, small white inclusions were observed on the monolith surface. The spent monoliths were more prone to brittle fracture. All these data suggest that the catalyst changes its physicochemical properties, probably including catalytic activity, under the ammonia oxidation conditions.

The purpose of this study is to understand why the oxide monolith catalyst IK-42-1 changes its properties in the course of long-term operation under industrial conditions. Finding out the causes of these changes taking place under the action of the reaction medium would help enhance the performance stability of the catalyst in ammonia oxidation.

EXPERIMENTAL

We studied the behavior of the commercial ammonia oxidation catalyst IK-42-1, which consists of 75% Fe_2O_3 (Mikhailovsky Chemical Reagent Plant, Malinovoe Ozero Village, Altai krai), 20% Al_2O_3, and 5% aluminosilicate fibers. The catalyst was shaped as 75 × 75 mm honeycomb monoliths 50 mm in height with 5 × 5 mm square-section channels and a wall thickness of 2 mm. The monolith calcination temperature was 950°C. The monoliths were used as the second-stage catalyst in a UKL-7 industrial reactor in the town of

Mendeleevsk. The first stage of the catalytic system consisted of nine gauzes made of the 81% Pt + 15% Pd + 3.5% Rh + 0.5% Ru alloy. Monoliths that had been on stream for 1500, 2504, or 3540 h were selected for examination. Both averaged catalyst samples and samples scraped off the monolith surface were analyzed.

Catalyst samples were characterized by chemical analysis, X-ray powder diffraction, mercury porosimetry, IR spectroscopy (including IR spectroscopy of probe molecules), secondary-ion mass spectrometry (SIMS), and temperature-programmed reduction (TPR).

The pore structure of catalyst samples was studied by mercury porosimetry using a Porosider-9300 instrument.

The specific surface area (S_{BET}, m^2/g) was determined by the BET method using argon thermal desorption.

X-ray diffraction patterns were obtained on an X'TRA (Thermo ARL, Switzerland) diffractometer (CuK_α radiation, $2\theta = 10°–80°$, 0.05-deg increments, counting time of 4 s per point). Interplanar spacings were determined using the Eva 10.0 program, a component of the software package supplied with Bruker D8 diffractometers. Unit cell parameters were refined by least squares using the Polikristall program [3].

Chemical analyses for platinum group metals were carried out on a BAIRD atomic absorption spectrometer. The metal detection limit was 0.001%.

The chemical composition of the catalyst surface was studied by SIMS on an MS-7201 mass spectrometer. The primary argon ion beam current was 0.6 μA, the beam diameter was 5 mm^2, and the ion energy was 4 keV. The ion intensities of elements were measured relative to the aluminum ion current for the reason that Al_2O_3 is sputtered congruently (without reduction) when bombarded by ions.

IR spectra were recorded on a BOMEM MB-102 spectrometer with 4-cm^{-1} resolution using the CsI pellet technique.

The nature of active sites on the catalyst surface was studied by IR spectroscopy of adsorbed probe molecules (NO). Diffuser reflectance spectra were recorded in the 400–4000 cm^{-1} range on a Bruker-IFS-113v Fourier spectrometer (4-cm^{-1} resolution, 100 co-added scans). NO was adsorbed at room temperature and a pressure of 20 Torr onto samples subjected to oxidative treatment at 300°C and then cooled and vacuumized.

Temperature-programmed reduction of catalyst samples (size fraction of 0.25–0.50 mm) was performed in a flow reactor fitted with a thermal-conductivity detector. Prior to reduction, the samples were conditioned in oxygen at 500°C for 3 h. The sample weight was 25 mg, and flow rate of the reducing mixture (10% H_2 + Ar) was 40 cm^3/min. The sample was heated to 900°C at a rate of 0.2 K/s.

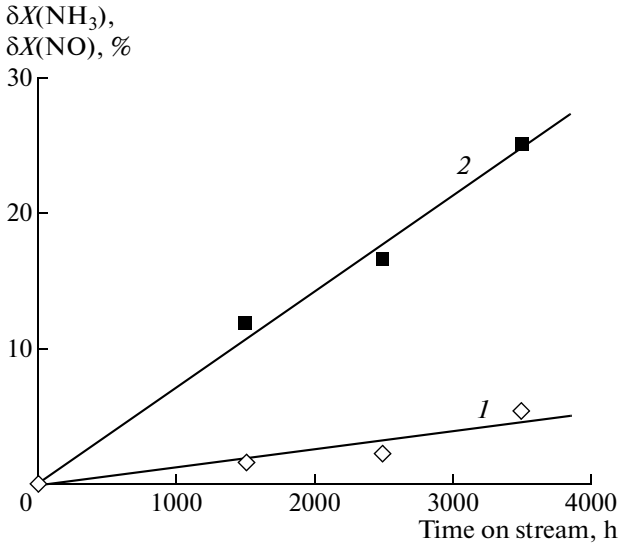

Fig. 1. Changes in the (*1*) ammonia conversion $\delta X(NH_3)$ and (*2*) nitrogen oxide yield $\delta X(NO)$ as a function of the catalyst time on stream.

The ammonia oxidation activity of the catalyst was determined in a flow reactor at atmospheric pressure in the temperature range of 700–900°C. The samples were monolith fragments 26 mm in diameter and ~50 mm in height. The ammonia–air mixture contained 5.0 ± 0.1% ammonia and was feed at a rate of 7.5 l/min. The ammonia and nitrogen oxide (NO, NO_2) concentrations were determined by on-line spectrophotometry [4]. At ammonia conversions close to 100%, the absolute error in this quantity was about 0.3%. The error in the nitrogen oxide concentrations did not exceed 6%. The change in the ammonia conversion was determined using the formula $\delta X(NH_3) = (X(NH_3)_{in} - X(NH_3)_{spent})/X(NH_3)_{in} \times 100\%$, and the change in the nitrogen oxide yield was calculated as $\delta X(NO) = (X(NO)_{in} - X(NO)_{spent})/X(NO)_{in} \times 100\%$, where $X(NH_3)_{in}$, $X(NO)_{in}$, $X(NH_3)_{spent}$, and $X(NO)_{spent}$ are the ammonia conversion and nitrogen oxide yield for the initial and spent catalysts, respectively (Fig. 1).

RESULTS AND DISCUSSION

Catalytic Activity

The changes in the activity and selectivity of the catalyst as a function of time on stream are plotted in Fig. 1. This data demonstrate that the activity (ammonia conversion) and NO selectivity of the catalyst in the industrial reactor decrease over time.

Note that the catalytic activity falls only slightly: the maximum decrease in the ammonia conversion is about 6% and is observed for the catalyst that has been on stream for 3540 h. At the same time, the nitrogen oxide yield falls significantly (by 25%). This can be

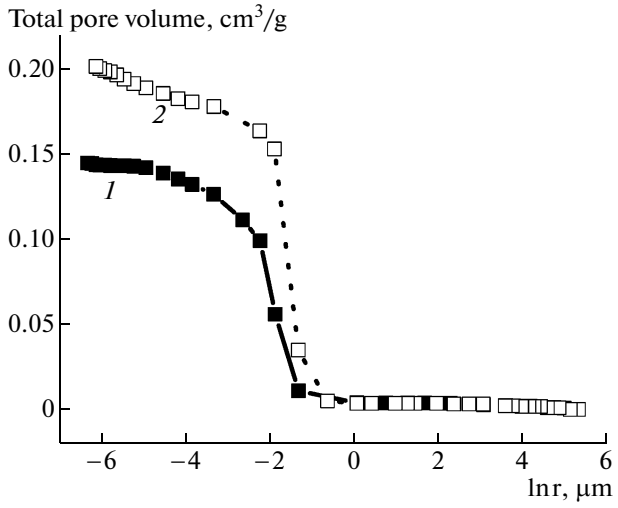

Fig. 2. Pore size distributions for the (*1*) initial and (*2*) spent catalysts. The time on stream is 3540 h; *r* is the pore radius.

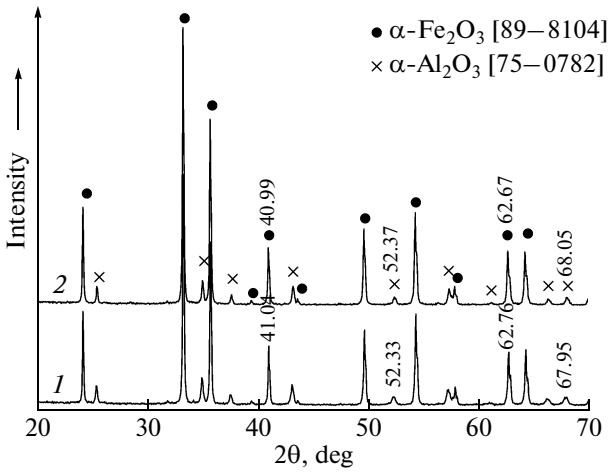

Fig. 3. X-ray diffraction patterns from the (*1*) initial and (*2*) spent catalysts.

caused by changes in the physicochemical properties of the catalyst (texture, phase composition, impurity composition, etc.) under the action of the reaction medium. The catalyst sample that had been on stream for the longest time (3540 h) was chosen for further studies because the properties of this sample were expected to be changed to the greatest extent.

Specific Surface Area and Pore Volume

Under the action of the reaction medium, the specific surface area of the catalyst decreases and the total pore volume increases. The initial catalyst has a specific surface area of 4.5 m^2/g and a total pore volume of 0.148 cm^3/g. After the reaction, the specific surface area of the catalyst is 2.7 m^2/g and its total pore volume is 0.204 cm^3/g. Figure 2 shows the pore size distributions for the initial and spent catalysts. Clearly, the mesopore volume in the spent catalyst is larger and the volume of macropores is almost unchanged. The observed decline in the mechanical strength of the monoliths upon their long-term operation can be attributed to this increase in the proportion of mesopores, which implies a decrease in the number of contact sites in the pellet and, possibly, microcracking.

Note that all of the spent catalyst samples, irrespective of the time on stream, have nearly equal specific surface areas and equal pore volumes. Therefore, the changes in the pore structure due to micropore sintering take place already in the initial 1500 h of catalyst operation.

Our earlier analysis of the texture of the catalyst samples as a function of the calcination temperature demonstrated the ammonia conversion is not correlated with the specific surface area or pore structure of the catalyst [5]. This is likely due to the fact that ammonia oxidation at high temperature is controlled by external diffusion, i.e., by the rate of the diffusion of the reacting gases to the outer (geometric) surface of the catalyst. Therefore, the observed slight decrease in the ammonia conversion at practically invariable monolith geometry can also be attributed to changes in the physicochemical properties of the catalyst and its surface.

X-Ray Diffraction Data

The initial catalyst is a mixture of the α-Fe_2O_3 and α-Al_2O_3 phases (Fig. 3). It was demonstrated earlier [5] that the components of the catalyst interact during catalyst preparation, yielding a solid solution of aluminum oxide in iron oxide. The changes in the unit cell parameters of aluminum oxide allow the formation of a solid solution of iron oxide in aluminum oxide, which was described in, e.g., [6].

The catalyst does not change its phase composition as it operates: the spent catalyst is also a mixture of the α-Fe_2O_3 and α-Al_2O_3 phases (Fig. 3). However, the reflections from both phases in the spent catalyst are shifted, indicating an increase in the unit cell volume of α-Fe_2O_3 (Table 1) and a decrease in the unit cell volume of α-Al_2O_3. The increase in the unit cell volume of the iron oxide phase can be due to a decrease in the aluminum content of the iron oxide phase, the hydration of the oxide yielding OH groups (protohematite phase), and the formation of oxygen vacancies. The decrease in the unit cell volume of α-Al_2O_3 can be caused by, e.g., by the loss of iron by the α-Al_2O_3-based solid solution.

IR Spectroscopic Data

Figure 4 presents the IR spectra of the surface layers of the initial and spent catalysts. The spectrum of the initial catalyst shows absorption bands characteris-

Table 1. Unit cell parameters and coherent-scattering domain (CSD) size for the initial and spent catalysts and, for comparison, the initial hematite

Unite cell parameter, pm; CSD, nm	Hematite α-Fe_2O_3	Initial catalyst		Spent catalyst	
		α-Fe_2O_3	α-Al_2O_3	α-Fe_2O_3	α-Al_2O_3
a	503.5(1)	501.8(1)	478.4(1)	502.2(1)	477.5(1)
c	1375.2(9)	1368.0(5)	1303.3(6)	1369.3(2)	1303.0(4)
CSD	>100	>150	85	>150	130

tic of α-Fe_2O_3: 347, 487, 566, and 810 cm^{-1} [7]. In the spectrum of the spent catalyst, the absorption band at 577 cm^{-1}, which is characteristic of the metal–oxygen bond vibrations, is shifted to lower frequencies relative to the same band for the initial catalyst. This shift is due to the shortening of the metal–oxygen bond, which can lead to an increase in the metal–oxygen bond energy, including for oxygen adsorbed on the catalyst surface. The change in the energy of bonding between adsorbed oxygen and the iron oxide catalyst surface is favorable for the reaction route yielding molecular nitrogen [8, 9]. In addition, the IR spectrum of the spent catalyst exhibits absorption bands at 384, 466, and 621 cm^{-1}, which are characteristic of spinel compounds, such as γ-Fe_2O_3, Fe_3O_4, and $FeAl_2O_4$.

Thus, the IR spectroscopic data suggest that Fe^{3+} in the surface layers of the catalyst undergoes partial reduction to Fe^{2+} under the industrial ammonia oxidation conditions to yield a spinel. This can be the cause of the observed decline in catalytic activity since only a low NO selectivity is observed in the presence of magnetite or iron aluminate [10]. The spinel can form from the hematite phase (e.g., by its reduction) and from the solid solution of iron in aluminum oxide. The formation of a spinel phase was not detected by X-ray diffraction. Therefore, either its content is below 5% or its particle size is very small. It is also possible that this phase does not form, but spinel-like defects are generated in the α-Fe_2O_3 structure.

Chemical Analysis

According to chemical analysis data, the surface of the spent monoliths contains platinum group metals, namely, platinum, palladium, and rhodium. The concentrations of these metals increase with time on stream and are 0.01, 0.001, and 0.03%, respectively, for the catalyst operated for 3540 h.

The most common industrial ammonia oxidation catalysts are gauzes made of platinum or its alloys with palladium and rhodium [11]. One of the causes of the deactivation of the platinum group metal gauzes is the loss of precious metals through evaporation and through the entrainment of metal particles as fine dust by the flowing gas. As a result, the gauze surface is enriched with rhodium, which is stabilized as the stable and nonvolatile oxide Rh_2O_3. This prevents the formation of an active chemisorbed oxygen layer, thus markedly slowing down the reaction between ammonia and oxygen and decreasing the nitrogen oxide selectivity [12–14].

The analysis of the oxide catalyst for precious metals indicates that the surface of the spent catalyst is enriched with rhodium. Because of its lower volatility, rhodium in oxide form is partially deposited on the catalyst, while platinum and palladium likely condense at lower temperatures. The deposition of rhodium oxide on the catalyst surface can be another cause of the decrease in the NO selectivity of the catalyst because rhodium catalyzes ammonia oxidation into nitrogen [15]. At the same time, the presence of rhodium can also change the surface properties of iron oxide.

SIMS Data

The composition of the catalyst surface was also studied by SIMS. The data obtained for penetration depths of <50 Å (surface layer) and 200 Å (subsurface layer) are presented in Table 2. The mass spectrum

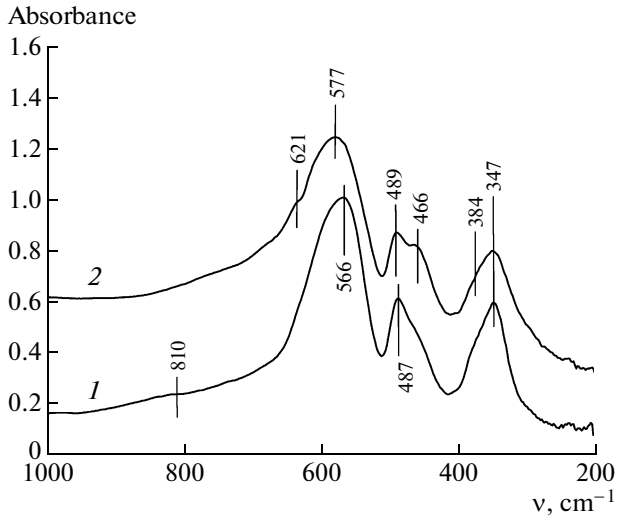

Fig. 4. IR spectra of the (*1*) initial and (*2*) spent catalysts.

Table 2. SIMS data for the surface (<50 Å) and subsurface (200 Å) layers of the initial and spent catalysts

Catalyst	Fe	Si	C	Na	Mg	K	Ca	Cr	Rh
Composition of the surface layer, <50 Å									
Initial	0.186	0.024	0.0015	0.009	–	0.005	0.033	0.0014	–
Spent	0.155	0.043	0.0020	0.060	0.0098	0.017	0.048	0.0053	0.003
Composition at a depth of ~200 Å									
Initial	0.125	0.022	–	0.002	0.0020	0.002	0.014	–	–
Spent	0.121	0.019	–	0.062	0.0034	0.011	0.015	0.0029	0.004

shows, along with ion currents of the major elements (Al, Fe, Si, O), ion currents due to alkali metals (Na, K), alkaline-earth metals (Mg, Ca), chromium, rhodium, and, in the surface layer, hydrocarbons (m/e = 12–15). A peak at $m/e = 83$ was detected for the bulk of the spent catalyst, which indicates the formation of the $FeAl^+$ ion. The appearance of this ion possibly indicates the formation of a spinel in the catalyst bulk. The increased intensities of the molecular ions FeH^+, $FeOH^+$, $AlOH^+$, and $SiOH^+$ from the surface layers of the spent catalyst are evidence that the catalyst surface is hydrated.

These data suggest that the surface layers of the spent catalyst contain increased concentrations of silicon, alkali and alkaline-earth metals, and chromium. The buildup of these elements is possibly due to the low purity of ammonia and air, which can contain various impurities, such as dross, silicates, particles of the iron–chromium catalyst for ammonia synthesis, oil, and dust [11].

The relative atomic concentration of rhodium is approximately 3% of the aluminum concentration and is nearly invariable in the surface and subsurface layers. The presence of rhodium in the subsurface layer can be due to its reaction with iron oxide, which possibly yields bimetallic compounds. There was a report in the formation of the stable compounds $LaRhO_3$, $MgRh_2O_4$, $YRhO_3$, and $RhTaO_4$ upon the calcination of supported rhodium catalysts at 950°C [16]. The rhodium content of the spent catalyst examined here is low, so such compounds could not be detected.

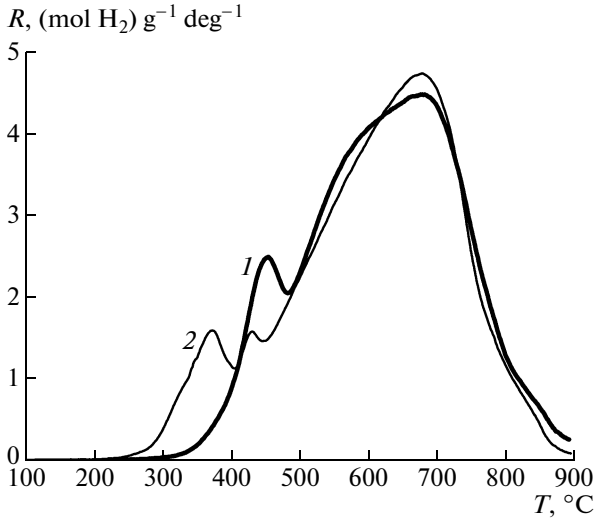

Fig. 5. TPR profiles of the (*1*) initial and (*2*) spent catalysts. *R* is the hydrogen uptake rate.

TPR Data

The near-surface samples of the initial and spent catalysts were examined by TPR, whose results are presented in Fig. 5.

The TPR profile of the initial catalyst conditioned in oxygen (curve *1*) indicates that the catalyst is reduced in two steps. The first peak arises from the reduction of Fe_2O_3 to Fe_3O_4, which takes place near 445°C. The second peak, occurring at ~670°C, is due to the further reduction of Fe_3O_4 to iron metal. These data are in good agreement with the α-Fe_2O_3 reduction data reported in the literature [17].

The TPR profile of the spent catalyst additionally exhibits a lower temperature peak at ~370°C and indicates a decrease in the $Fe_2O_3 \rightarrow Fe_3O_4$ conversion temperature to ~425°C. The peak at 370°C can be due to, e.g., rhodium oxide reduction. It was demonstrated by other authors that the α-Fe_2O_3 reduction temperature can be varied by introduction of various admixtures, such as copper and nickel oxides. Therefore, the enrichment of the surface of the spent catalyst with chromium and rhodium compounds can facilitate the reduction of this catalyst by hydrogen.

The noticeably lower $Fe_2O_3 \rightarrow Fe_3O_4$ conversion temperature for the spent catalyst as compared to the initial catalyst, which indicates that the magnetite phase forms more readily during reduction, can also be due to the formation of spinel-like defects in the hematite phase via partial oxygen loss from the oxide. This shortens the nucleation time for the new phase and leads immediately to the growth of the nuclei. This assumption is corroborated by the hydrogen uptakes for the low-temperature peaks of the initial and spent catalysts, which were estimated to be 0.31 ×

10^{-2} and 0.26×10^{-2} (mol H_2)/(g Cat), respectively. The total hydrogen uptake was 1.31×10^{-2} and 1.24×10^{-2} (mol H_2)/(g Cat), respectively.

NO Adsorption

The state of iron cations on the catalyst surface was characterized by IR spectroscopy of adsorbed NO as probe molecules. The spectra of NO adsorbed on the surface of the initial and spent catalysts are shown in Fig. 6. Both spectra consist of several incompletely resolved absorption bands.

NO adsorption on the surface of the initial sample gives rise to absorption bands at 1809 and 1885 cm^{-1}. The 1885 cm^{-1} band is due to NO adsorbed on coordinative unsaturated Fe^{2+} cations ($(O_5)Fe^{2+}$–NO) in the hematite phase. The band at 1809 cm^{-1} is likely assignable to the $(O_{5-x})Fe^{2+}$–NO complexes, in iron is in a nearly tetracoordinated state. These iron cations with small coordination numbers down to 4 (clustered cations) can likely appear in the solid solution of iron oxide in aluminum oxide [18]. Similar absorption bands were observed for NO adsorbed on alumina-supported iron oxide [19].

Note that, for the given catalyst, we did not observe absorption bands characteristic of NO adsorption on Fe^{2+}–O–Fe^{3+} sites, which would occur in the 1930–1950 cm^{-1} range. At the same time, at longer wavelengths we observed a number of bands indicating the formation of various nitrite–nitrate complexes on the oxide surface: see the absorption band with a maximum at 1550 cm^{-1} and inflections at 1590 and 1630 cm^{-1}. The appearance of these features along with the reduced adsorption sites suggests that the catalyst surface interacts strongly with the adsorbed NO molecules to yield the reduced adsorption sites and nitrates.

According to an earlier study [18], ammonia oxidation can take place not only on the coordinatively unsaturated sites of the hematite phase, but also on Fe^{2+} sites in a nearly tetracoordinated state (absorption band near 1810 cm^{-1}), which form from iron cations of the solid solution of iron oxide in aluminum oxide.

For the spent catalyst, the spectrum of adsorbed NO shows only two major absorption bands indicating NO adsorption on low-coordinated/clustered Fe^{2+} sites (1813 cm^{-1}) and the formation of nitrite–nitrate complexes (1545 cm^{-1}). The lower intensity of the 1813 cm^{-1} band is evidence that the number of reduced, coordinatively unsaturated sites on the surface of the spent catalyst is much smaller than the number of these sites on the surface of the initial catalyst (with the change in the specific surface area taken into account). The fact that the spent catalyst has a smaller number of these reduced sites on its surface in spite of its better reducibility, established by TPR, can be due to the recrystallization of the α-Al_2O_3-based solid solution of iron and the formation of a spinel.

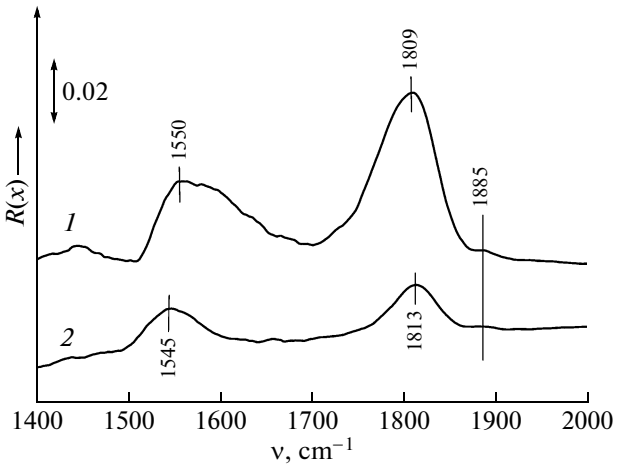

Fig. 6. IR spectra of adsorbed NO (20 Torr) on the surface of the (*1*) initial and (*2*) spent catalysts.

Another possible cause of this fact, which would account for the absence of the absorption band at 1885 cm^{-1}, is the blocking of part of the active sites on the surface by compounds of silicon, alkali and alkaline-earth metals, chromium, rhodium, etc.

Our data are in agreement with the results of an earlier study [18] that demonstrated that the catalyst having a higher concentration of coordinatively unsaturated adsorption sites or a higher reactivity toward NO (that is, a higher concentration of nitrate complexes) will be more selective in ammonia oxidation. In the spent catalyst, the surface is blocked under the action of the reaction medium and the solid solution of iron oxide in aluminum oxide is broken down. This causes a decrease in the number of active sites. Accordingly, the spent catalyst affords a lower nitrogen oxide yield than the initial catalyst.

CONCLUSIONS

The comparative study of the initial and spent IK-42-1 catalyst samples demonstrated that, during ammonia oxidation, the catalyst surface is enriched with silicon and alkali and alkaline-earth metal ions, which can stabilize a local spinel-like structure, and with chromium ions. The buildup of these elements can be due to the insufficient purity of the reacting gases. The surface of the spent catalyst contains platinum group metals as well (Pt < Pd < Rh), whose content depends on the time on stream because these metals are permanently lost by the platinum metal gauzes. No significant changes in the phase composition of the catalyst were observed.

The observed decrease in the mechanical strength of the monoliths is due to the changes in the textural properties of the catalyst, primary its pore structure, because of sintering taking place at high temperatures.

The ammonia conversion is almost constant in time because of the invariable geometry of the catalyst.

The slightly lower ammonia conversion on the spent catalyst can be due to this catalyst having smaller accessible surface area because of surface blocking or a decrease in the specific surface area. This indicates that the reaction under laboratory test conditions can take place in part on the inner surface of the catalyst.

The significant change in the selectivity of the catalyst can be due to both the change in the impurity composition (silicon, alkali metal, alkaline-earth metal) and the formation of spinel-like defects in the hematite phase or the conversion of the solid solution of iron in aluminum oxide into iron aluminate. These processes lead to a lower concentration of active, coordinatively unsaturated Fe^{2+}, adsorption sites responsible for ammonia oxidation into NO.

Therefore, the high initial selectivity of the catalyst can be conserved by improving the process, primarily through deeper purification of the reacting gases (air and ammonia), and by raising the stability of the catalyst, for example, by stabilizing the hematite phase and the solid solution of iron oxide in aluminum oxide.

REFERENCES

1. Sadykov, V.A., Brushtein, E.A., Isupova, L.A., et al., *Khim. Prom–st.*, 1997, vol. 12, p. 33.
2. Chernyshev, V.I. and Brushtein, E.A., *Katal. Prom–sti.*, 2001, no. 3, p. 30.
3. Tsybulya, S.V., Cherepanova, S.V., and Solov'eva, L.P., *Zh. Strukt. Khim.*, 1996, vol. 37, no. 2, p. 379.
4. Sutormina, E.F, *Zh. Anal. Khim.*, 2004, vol. 59, no. 4, p. 373 [*J. Anal. Chem.* (Engl. Transl.), vol. 59, no. 4, p. 331].
5. Kruglyakov, V.Yu., Isupova, L.A., Kulikovskaya, N.A., et al., *Katal. Prom–sti.*, 2007, no. 2, p. 46.
6. Kirichenko, O.A., Ushakov, V.A., Moroz, E.M., and Vorob'eva, M.P., *Kinet. Katal.*, 1993, vol. 34, no. 4, p. 739.
7. Yurchenko, E.N., Kustova, T.N., and Batsanov, S.S., *Kolebatel'nye spektry neorganicheskikh soedinenii* (Vibrational Spectra of Inorganic Compounds), Novosibirsk: Nauka, 1981.
8. Ryabchun, A.A., Savenkov, A.S., and Nikityuk, A.V., *"Catalysis on the Eve of the XXI Century: Science and Engineering," The Second Int. Memorial Boreskov Conf.*, Novosibirsk, 1997, part 2, p. 200.
9. Savenkov, A.S., Ryabchun, A.A., Atroshchenko, V.I., and Gromov, D.A., *Nestatsionarnye protsessy v katalize* (Unsteady-State Processes in Catalysis), Novosibirsk, 1986, issue 3, p. 134.
10. Zakharchenko, N.I., *Izv. Vyssh. Uchebn. Zaved., Khim. Khim. Tekhnol.*, 2001, no. 2, p. 127.
11. *Katalizatory v azotnoi promyshlennosti* (Catalysts in the Nitrogen Industry), Atroshchenko, V.I., Ed., Kharkov: Visshcha Shkola, 1977.
12. Schmidt, L.D. and Luss, D., *J. Catal.*, 1971, vol. 22, p. 262.
13. Contor, J.P., Mouvier, G., Hoogewys, M., and Leclere, G., *J. Catal.*, 1977, vol. 48, p. 217.
14. Zabrzeski, J. and Zmyslony, R., *Appl. Catal.*, 1987, vol. 35, p. 13.
15. Li, Y. and Armor, J.N., *Appl. Catal., B*, 1997, vol. 13, no. 2, p. 131.
16. Ruckenstein, E. and Wang, H.Y., *J. Catal.*, 2000, vol. 190, p. 32.
17. Shimokawabe, M., Furuichi, R., and Ishii, T., *Thermochim. Acta*, 1979, vol. 28, p. 287.
18. Isupova, L.A., Budneva, A.A., Kruglyakov, V.Yu., and Paukshtis, E.A., *Kinet. Katal.*, 2009, vol. 50, no. 2, p. 280 [*Kinet. Catal.* (Engl. Transl.), vol. 50, no. 2, p. 264].
19. Davydov, A.A., *IK-spektroskopiya v khimii poverkhnosti okislov* (IR Spectroscopy Applied to the Chemistry of Oxide Surfaces), Novosibirsk: Nauka, 1984.